

# Fabrication of chitosan–magnetite nanocomposite strip for chromium removal

Vaishnavi Sureshkumar<sup>1</sup> · S. C. G. Kiruba Daniel<sup>1</sup> · K. Ruckmani<sup>2</sup> · M. Sivakumar<sup>1</sup>

Received: 18 February 2015 / Accepted: 6 March 2015 / Published online: 22 March 2015  
© The Author(s) 2015. This article is published with open access at Springerlink.com

**Abstract** Environmental pollution caused by heavy metals is a serious threat. In the present work, removal of chromium was carried out using chitosan–magnetite nanocomposite strip. Magnetite nanoparticles ( $\text{Fe}_3\text{O}_4$ ) were synthesized using chemical co-precipitation method at 80 °C. The nanoparticles were characterized using UV–visible spectroscopy, fourier transform infrared spectroscopy, X-ray diffraction spectrometer, atomic force microscope, dynamic light scattering and vibrating sample magnetometer, which confirm the size, shape, crystalline nature and magnetic behaviour of nanoparticles. Atomic force microscope revealed that the particle size was 15–30 nm and spherical in shape. The magnetite nanoparticles were mixed with chitosan solution to form hybrid nanocomposite. Chitosan strip was casted with and without nanoparticle. The affinity of hybrid nanocomposite for chromium was studied using  $\text{K}_2\text{Cr}_2\text{O}_7$  (potassium dichromate) solution as the heavy metal solution containing Cr(VI) ions. Adsorption tests were carried out using chitosan strip and hybrid nanocomposite strip at different time intervals. Amount of chromium adsorbed by chitosan strip and chitosan–magnetite nanocomposite strip from

aqueous solution was evaluated using UV–visible spectroscopy. The results confirm that the heavy metal removal efficiency of chitosan–magnetite nanocomposite strip is 92.33 %, which is higher when compared to chitosan strip, which is 29.39 %.

**Keywords** Magnetite nanoparticles · Chitosan · Chitosan–magnetite nanocomposite strip · Chromium

## Introduction

Heavy metals like Hg (II), Pb (II), Cd (II) and Cu (II) are harmful because they are non-biodegradable in nature, long half-life, and get accumulated in different parts resulting in environmental pollution, of which, chromium is one of the most lethal heavy metal. Chromium exists in two forms namely the trivalent (III) and hexavalent (VI) form. Cr(VI) is considered to be more carcinogenic. The industrial sources of Cr(VI) primarily include alloy and steel manufacturing, metal finishing, electroplating, leather tanning, pigments and dyeing industries. The effluents from these industries contain Cr(III) and Cr(VI) at concentrations ranging from tenths to hundreds of ppm (Mcbain et al. 2008). Hexavalent chromium usually exists in water as oxyanions such as chromate ( $\text{CrO}_4^{2-}$ ) and dichromate ( $\text{Cr}_2\text{O}_7^{2-}$ ) and does not precipitate easily using the conventional methods (Campo et al. 2005).

There are a number of methods reported for the removal of heavy metals, such as ion exchange (Deng et al. 2005), filtration (Chen et al. 2005), precipitation (Chang and Chen 2005), membrane process, reverse osmosis (Xu et al. 2012), sedimentation and electrochemical treatment (Kim et al. 2001). Out of all the process, the membrane adsorption technique is the most preferable one for heavy

V. Sureshkumar and S. C. G. Kiruba Daniel contributed equally.

✉ K. Ruckmani  
hodpharma@gmail.com

✉ M. Sivakumar  
muthusiva@gmail.com

<sup>1</sup> Division of Nanoscience and Technology, Anna University, BIT campus, Tiruchirappalli, India

<sup>2</sup> Department of Pharmaceutical Technology, DST Sponsored National Facility for Drug Development for Academia, Pharmaceutical and Allied Industries, Anna University, BIT Campus, Tiruchirappalli 620024, Tamilnadu, India

metal ion removal. There are a variety of bio-adsorbents, but these bio-adsorbents have low adsorption capacities and slow process kinetics. So, there is a need to develop an innovative adsorbent useful for industry and which is eco-friendly.

Chitosan is being utilized for water purification process for a long time because of its properties such as polymeric nature, biodegradable and non-toxic. It is the second most abundant material in the environment next to cellulose. Chitosan has amine functional group that reacts strongly with metal ions and has a high potential of removing heavy metals as it binds the metal ions easily. The main objective of the present work was (i) to remove Cr(VI) from aqueous solution, (ii) to show that the removal efficiency of chromium by chitosan–magnetite nanocomposite strip is greater, (iii) to prove that the nanocomposite strip is a cost-effective and simple process. It is proposed here to make nanocomposite strip using chitosan and magnetite nanoparticles. Chitosan–magnetite nanocomposite strip follows physicochemical adsorption process to remove Cr(VI). The unique properties of magnetite nanoparticles are they have high surface area–volume ratio, extremely small size, surface modifiability, excellent magnetic properties and great biocompatibility. Earlier studies have been done on magnetite nanoparticles to investigate its adsorption capacity towards heavy metals (Martínez-Mera et al. 2007; Yuan et al. 2010; Adikary and Sewvandi 2011). Also, chitosan, a biopolymer, which is extracted from crustacean shells or from fungal biomass, has high porosity resulting in superior binding properties for metal ion such as cadmium, copper, lead, uranyl, mercury and chromium (Zheng et al. 2007; Han et al. 2012; Recep and Ulvi 2008; Shilpi et al. 2011; Yue et al. 2011). Magnetite nanoparticles with chitosan would possibly have better heavy metal removal. Hence, it is planned that magnetic nanoparticles could be introduced in chitosan for the heavy metal removal in aqueous stream. The synergistic effect of chitosan along with magnetite nanoparticles in removing chromium has also been studied in this report.

## Materials and methods

Reagents such as ferrous sulphate ( $\text{Fe}_2\text{SO}_4 \cdot 7\text{H}_2\text{O}$ ), ferric chloride ( $\text{FeCl}_3 \cdot 6\text{H}_2\text{O}$ ), sodium hydroxide ( $\text{NaOH}$ ), potassium dichromate ( $\text{K}_2\text{Cr}_2\text{O}_7$ ) and glacial acetic acid (99% pure) were purchased from Sigma-Aldrich with high purity. Chitosan [mol. wt: 375 kDa, viscosity: 200–800 Kcps; 90 % deacetylated; soluble in dilute aqueous acid ( $\text{pH} < 6.5$ )] is also purchased from Sigma-Aldrich. Synthesized nanoparticles were characterized by UV–visible spectrophotometer (JASCO V 650), Fourier transform infrared spectroscopy–Perkin Elmer Spectrum RX I FTIR

instrument, X-Ray diffraction–Rigaku Ultima III XRD, dynamic light scattering–Malvern Zetasizer V 6.20 series, atomic force microscope–Park AFM XE-100 and vibrating sample magnetometer–VSM model 7404, respectively. The casted chitosan–magnetite strip was characterized using FESEM EDX instrument. Heavy metal ion-removed aqueous samples were analysed using UV–visible spectrophotometer (JASCO V 650).

## Synthesis of magnetite nanoparticles ( $\text{Fe}_3\text{O}_4$ )

Magnetite ( $\text{Fe}_3\text{O}_4$ ) nanoparticles were synthesized by chemical co-precipitation method. The concentrations of ferrous sulphate:ferric chloride precursors are 0.75 M each. The precursors are taken in 2:1 ratio and stirred well for 15 min. After 15 min of stirring, sodium hydroxide is added at regular intervals to the precursor solution. Upon addition of  $\text{NaOH}$ , the solution turned black, indicating the formation of magnetite nanoparticles. Further stirring is continued for 1 h to uniformly disperse the magnetic nanoparticles. The nanoparticles were centrifuged and washed with deionised water. The magnetite powder obtained was then dispersed into deionised water and used for the experiment (Fig. 1). The entire reaction is given by the equation as follows:



## Fabrication of Chitosan–magnetite nanocomposite strip

One wt% of chitosan is dissolved in 1 vol% glacial acetic acid. The chitosan solution was sonicated for 15 min, and the solution was allowed to stir for 18 h. 0.05 g of magnetite nanoparticles was added to the chitosan solution and stirred again for 6 h to get chitosan–magnetite

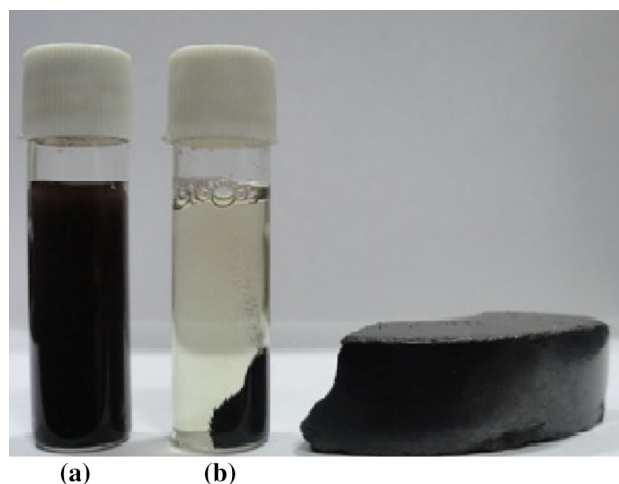


**Fig. 1** Magnetite nanoparticles (a) Magnetite nanoparticles attracted by an external magnet (b)

**Fig. 2** Schematic representation of fabrication of hybrid strip (chitosan–magnetite nanocomposite) using solution casting method

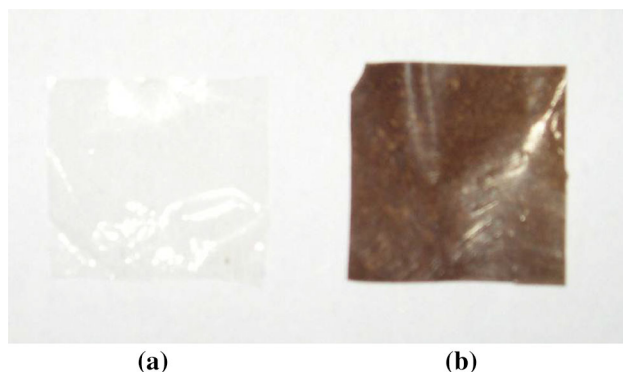
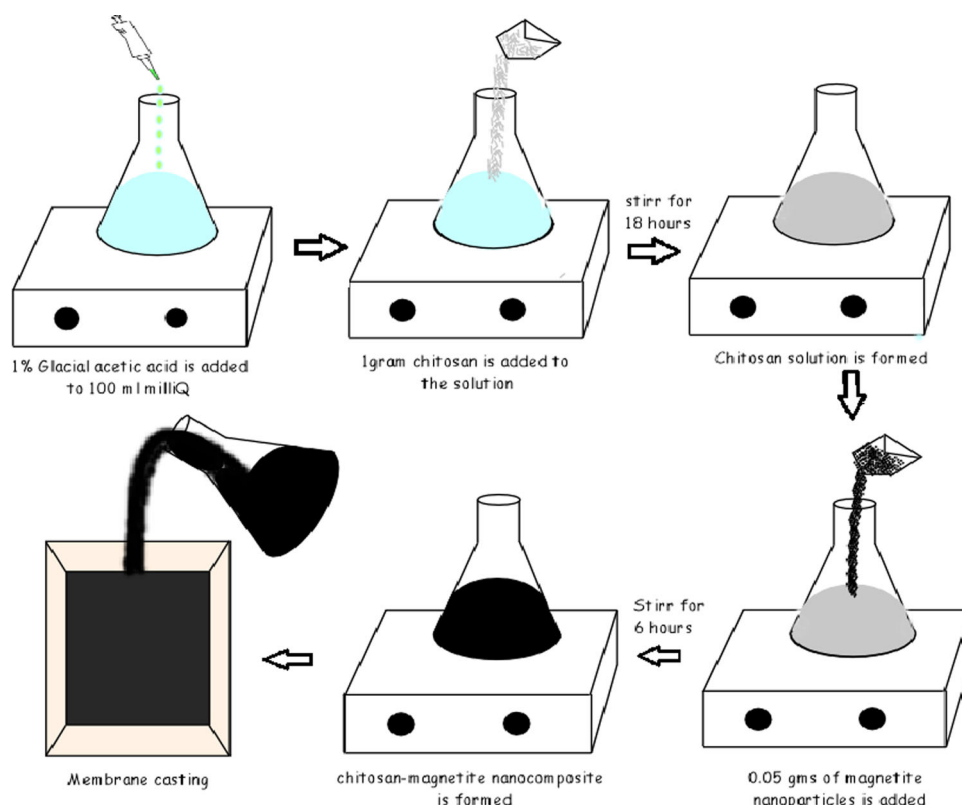


**Fig. 3** Colour variation of chitosan strip (a) when compared to chitosan–magnetite nanocomposite strip (b)

nanocomposite solution. Similarly, plain chitosan solution was also prepared as control. Both the solutions were then casted onto petriplate and were allowed to dry at room temperature for 48 h. The preparation of hybrid strip is shown in Fig. 2. Chitosan strip and Chitosan–magnetite nanocomposite strip were then peeled off from the petriplate and were cut into 1 cm × 1 cm and were used for further analysis (Fig. 3).

### Adsorption experiments

The removal of heavy metals from the aqueous solution was studied using chitosan strip and chitosan–magnetite

nanocomposite strip. Aqueous solution of chromium was prepared from potassium dichromate ( $K_2Cr_2O_7$ ). The concentration of the heavy metal solution is 5 mM in 30 ml deionised water. The aqueous solution (30 ml) was prepared and divided into 10 ml each. The chitosan strip and nanocomposite strip cut into 1 cm × 1 cm are dropped in 10 ml solution each. The adsorption experiments were carried out, and the reduction in the concentration of the aqueous solution was recorded at regular time intervals. The chitosan and nanocomposite strip swell, indicating that the heavy metal ions are adsorbed onto the strip. The heavy metal removal efficiency of chitosan strip and nanocomposite strip was evaluated using UV–visible spectroscopy.

## Results and discussion

### UV–visible and FTIR spectroscopy

Iron oxides, such as magnetite, exhibit thermally induced electron delocalization between  $Fe^{2+}$  and  $Fe^{3+}$  ions. The UV–visible peak for magnetite nanoparticles was obtained at 407 nm (Fig. 4). The reported UV–visible peak was found to be 404 nm (Rahman et al. 2011), and result obtained in the experiment was 407 nm. From the data obtained, the peak in the near IR region confirms the presence of magnetite ( $Fe_3O_4$ ) nanoparticles. When magnetite is

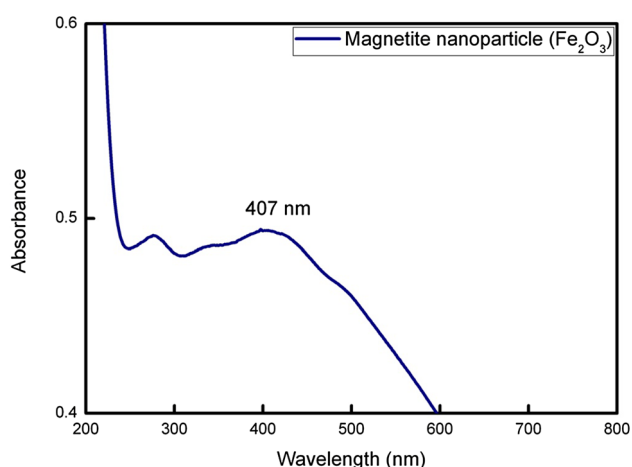


**Fig. 4** UV–visible absorption spectroscopic analysis of the synthesized magnetite nanoparticles exhibiting peak at 407 nm

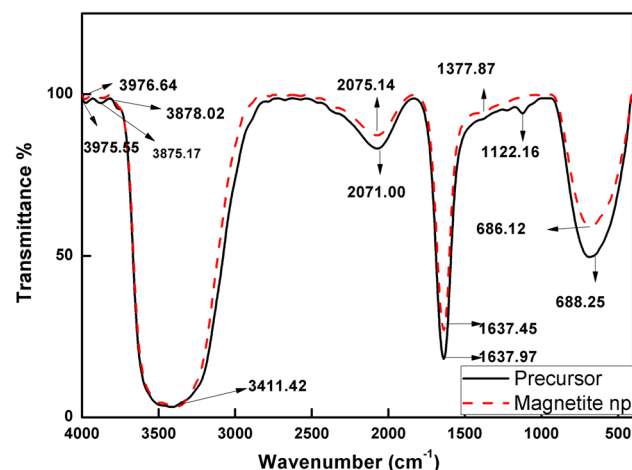


**Fig. 5** FTIR analysis of the precursor solution (ferrous sulphate:ferrous chloride) and magnetite nanoparticles

oxidized, it becomes maghemite nanoparticles and the UV–V peak is expected to decrease because of no absorption in the near IR region.

FTIR was analysed for the ferric chloride:ferrous sulphate mixture and  $\text{Fe}_3\text{O}_4$  nanoparticles (Fig. 5). The strong absorption band at  $684\text{ cm}^{-1}$  is assigned to the vibrations of the Fe–O bond, which confirm the formation of  $\text{Fe}_3\text{O}_4$  nanoparticles. Previously, it was reported that the characteristic absorption band for Fe–O in bulk  $\text{Fe}_3\text{O}_4$  appeared at 570 and  $375\text{ cm}^{-1}$  wavenumber (Waldon 2008). However, in the present case, the band for Fe–O shifts towards higher wavenumber<sup>18</sup> of  $686\text{ cm}^{-1}$ . It is due to the breaking of the large number of bands for surface atoms, resulting in the rearrangement of localized electrons on the particle surface, and the surface bond force constant increases as  $\text{Fe}_3\text{O}_4$  is reduced to nanoscale dimension, so that the absorption bands shift to higher wavenumber. The broad absorption at

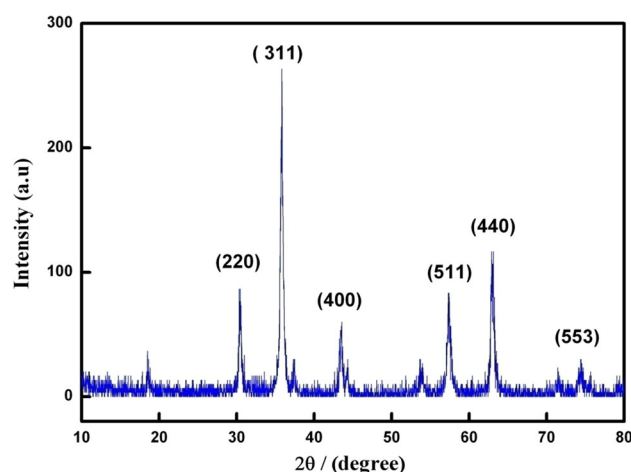


**Fig. 6** X-ray diffraction analysis for the synthesized magnetite nanoparticles exhibiting characteristic peaks of plane (311) of matching with JCPDS file no: 19-0629

$3421\text{ cm}^{-1}$  corresponds to the overlapping stretching vibrations of aromatic  $\text{OH}^-$  group and aromatic hydrogen and NH groups. The wavenumber at  $1646\text{ cm}^{-1}$  corresponds to C=O stretching vibration (Shilpi et al. 2011).

### X-Ray diffraction analysis

Figure 6 illustrates the XRD patterns of magnetic nanoparticles. It is clear from the graph that only the  $\text{Fe}_3\text{O}_4$  phase is of highly crystalline nature. The position and relative intensity of all diffraction peaks match well with those of the magnetite (JCPDS file no: 19-0629), and broad peaks indicate the nano-crystalline nature of the particles (Guin and Manorama 2008) having face-centred cubic inverse spinel structure. No peaks of any other phases are observed in the XRD patterns, indicating the high purity of the products. As reported earlier (Pattnaik 2011), black colour of the nanoparticles indicates the presence of magnetite phase and not maghemite phase. The diffraction peak (311) plane corresponds to the magnetite nanoparticles; the  $2\theta$  value is  $35.7^\circ$ .

### Stability of magnetite nanoparticles

Zeta potential indicates the degree of repulsion between adjacent, similarly charged particles in the dispersion and the stability of the particles in the dispersion. The zeta potential value of the  $\text{Fe}_3\text{O}_4$  nanoparticles was found to be  $-16.5\text{ mV}$  (Fig. 7). Report indicates that the magnetite nanoparticles are stable in the dispersion.

### Morphology of magnetite nanoparticles

To investigate the morphology and monodispersity of magnetite nanoparticles, AFM analysis has been done.

**Fig. 7** Zeta potential analysis of the synthesized magnetite nanoparticles exhibiting value of  $-16.5$  mV

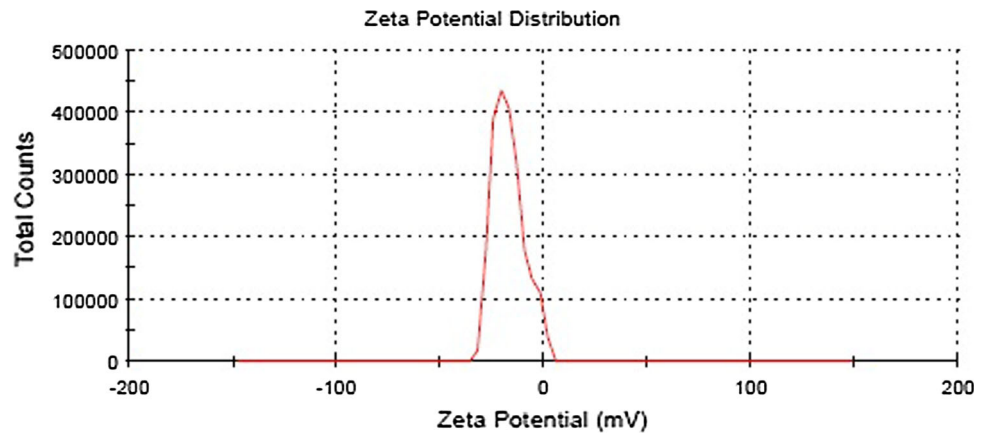
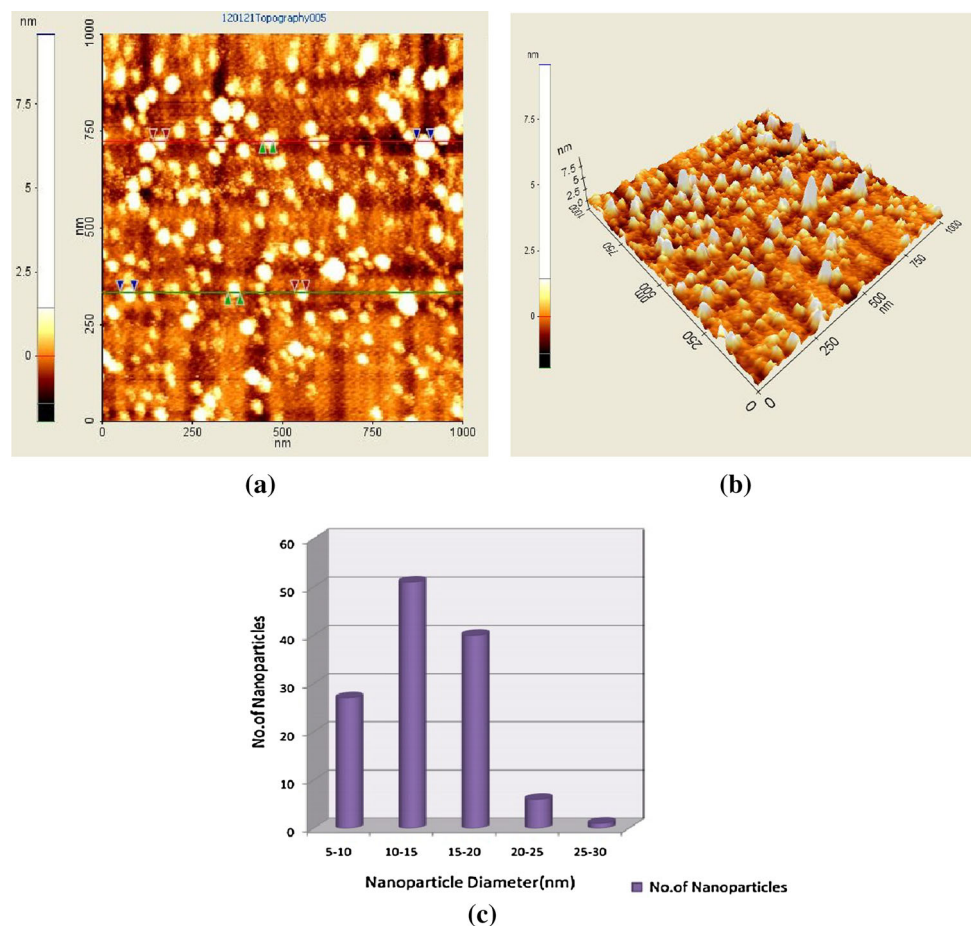


**Fig. 8** 2D atomic force microscopic image of  $\text{Fe}_3\text{O}_4$  nanoparticles (a) 3D atomic force microscopic image of  $\text{Fe}_3\text{O}_4$  nanoparticles (b) Histogram of magnetite nanoparticles (c)



Both two-dimensional and three-dimensional images of magnetite nanoparticles were obtained (Fig. 8). The magnetite nanoparticles characterized by AFM reveal that the particle sizes are uniformly distributed. The particle size was found to be around 10–20 nm. The magnetite nanoparticles were uniformly distributed. The AFM results matched with the previously published reports having a size of 35 nm, respectively (Cai and Wan

2007). AFM image is analysed using J image software to interpret the diameter of individual nanoparticle. The cumulative result is then plotted as a histogram. The results show that the nanoparticles are spherical in shape. From the histogram data, the number of nanoparticles in each size range has been found, with a maximum number of nanoparticles having a size of 10–15 nm.



## Magnetic behaviour of magnetite nanoparticles

Vibrating sample magnetometer predicts the magnetic behaviour of nanoparticles. Figure 9 gives the magnetization loop for magnetite nanoparticles at room temperature. The magnetic hysteresis curve exhibits the superparamagnetic behaviour. The material exhibits a narrow hysteresis curve with a small value of coercivity and retentivity. VSM results show that the coercivity ( $H_{ci}$ ), which is the field required to magnetize the material, is 61.172 Oe and retentivity ( $M_r$ ), which is the field required to demagnetize the material, is 5.4324 emu/g. The saturation magnetization value of the magnetite nanoparticles was found to be 70.787 emu/g, which indicates that above this value, the material cannot be magnetized. The above-obtained results corroborated with the earlier reports (Sundrarajan and Ramalakshmi 2012), where the magnetization value is 41.5 emu/g. From the hysteresis loop obtained, it is clear that magnetite nanoparticle has the properties of a soft magnet that can easily magnetize and demagnetize.

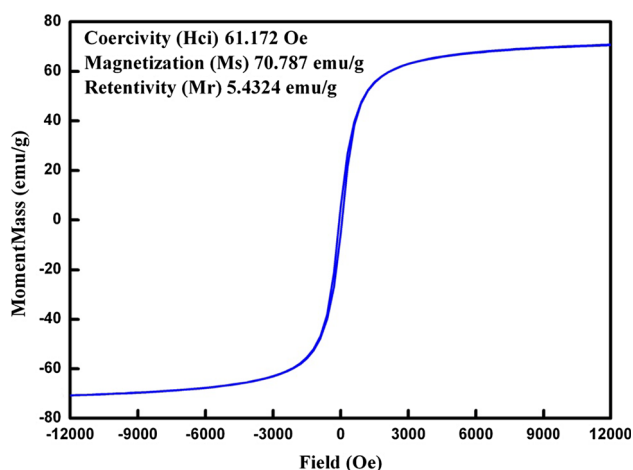
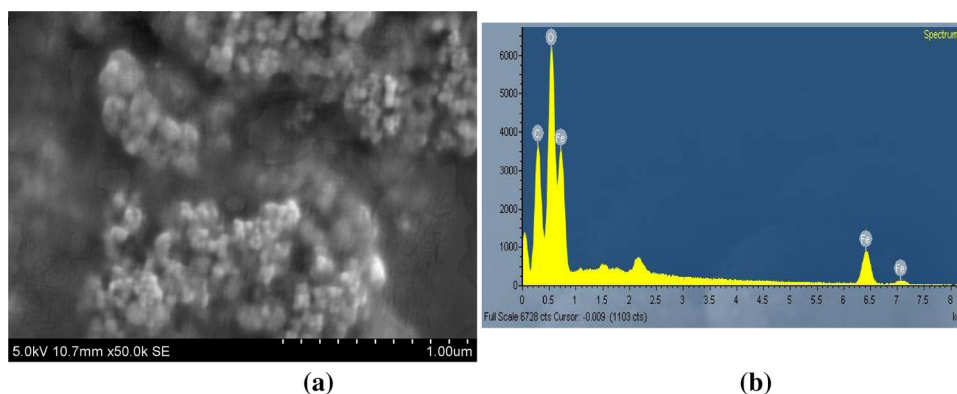


**Fig. 9** Vibrating sample magnetometer analysis of magnetite nanoparticles exhibiting the coercivity ( $H_{ci}$ ) and retentivity ( $M_r$ ) value of magnetite nanoparticles as 61.172 Oe and 5.4324 emu/g, respectively

**Fig. 10** FESEM image of chitosan–magnetite nanocomposite strip (a) EDX spectra of nanocomposite strip (b)



## FESEM–EDX analysis for nanocomposite strip

The FESEM results (Fig. 10a) show that the nanoparticles are distributed in the chitosan strip. The nanoparticles are spherical in shape and are evenly distributed. The number and energy of the X-rays emitted from a specimen can be measured by an energy-dispersive spectrometer. The electron dispersive spectroscopy (EDS) analysis of these particles indicates the presence of Fe and O composition in the chitosan–magnetite nanocomposite strip (Fig. 10b). The elemental composition of iron, oxygen and carbon is 52.71, 34.88 and 43.54 %, respectively. The results obtained matched with the previous reports, where the composition of iron and oxygen in iron oxide nanoparticles was found to be 54.11 and 45.88 %, respectively. No other peak related to any impurity has been detected in the EDS, which confirms that the grown nanoparticles in the nanocomposite strip are composed only with iron and oxygen and carbon. Thus, the presence of iron content in the nanocomposite strip was confirmed from the EDX results.

## Studies on Cr(VI) removal

The removal of chromium [Cr(VI)] ions from the aqueous solution was evaluated using chitosan–magnetite nanocomposite and chitosan strips. Chitosan strip is kept as the control. Due to the better dispersion performance of magnetite nanoparticles, they are chosen for the adsorption tests in this study. The removal of Cr (VI) was done using UV–visible absorption spectrophotometer (JASCO V 650) at different time intervals (Fig. 11). From the values of absorbance obtained, it is known that chitosan removes chromium ions, but chitosan–magnetite nanoparticles were highly efficient in the removal of chromium ions [Cr(VI)]. From this, it is clear that the nanocomposite has a greater efficiency than chitosan strip in the removal of chromium (VI). The graph obtained, when compared to earlier studies<sup>3</sup>, shows that chromium uptake by  $Fe_3O_4$  nanoparticles is a physicochemical process, including electrostatic

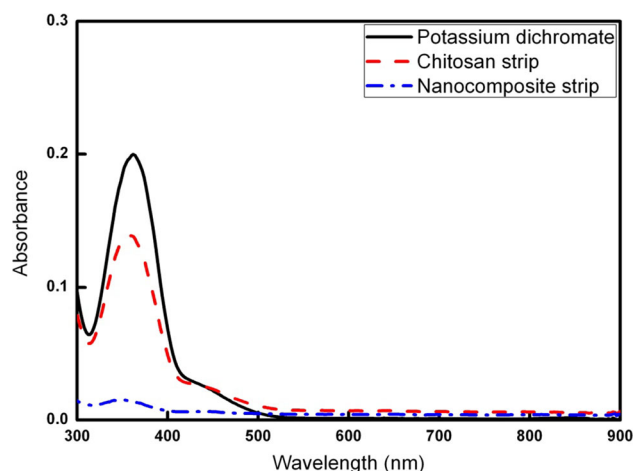


**Fig. 11** UV-visible spectroscopic analysis of removal of chromium from the aqueous solution by hybrid strip

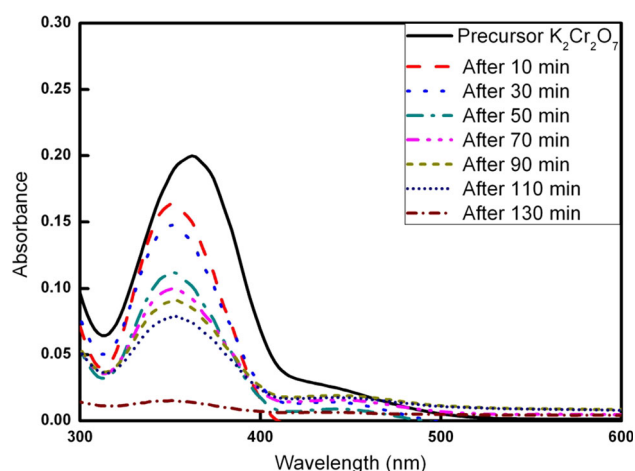


**Fig. 12** UV-visible spectroscopic results for the adsorption kinetics of Cr(VI) removal using nanocomposite strip at regular time intervals

interaction followed by redox process where the Cr(VI) is reduced to Cr(III). Adsorption kinetics was studied to understand the removal of Cr(VI) ions from  $K_2Cr_2O_7$  solution (Fig. 12). UV-visible spectroscopic results were obtained for the aqueous heavy metal solution, and it was compared with the chitosan-magnetite nanocomposite strip at regular time intervals such as 10, 30, 50, 70, 90, 110 and 130 min, respectively. Maximum adsorption of Cr(VI) is obtained at 130 min. The regular decrease in the value of absorbance shows the removal of Cr(VI) ions at each time interval. The removal of efficiency of chitosan and chitosan-magnetite nanocomposite strip is plotted against time in Fig. 13. From the above results, it is noted that the removal efficiency of chitosan strip is 29.39 %, and that of the chitosan-magnetite nanocomposite strip is 92.33 %. The removal efficiency is calculated using the formula

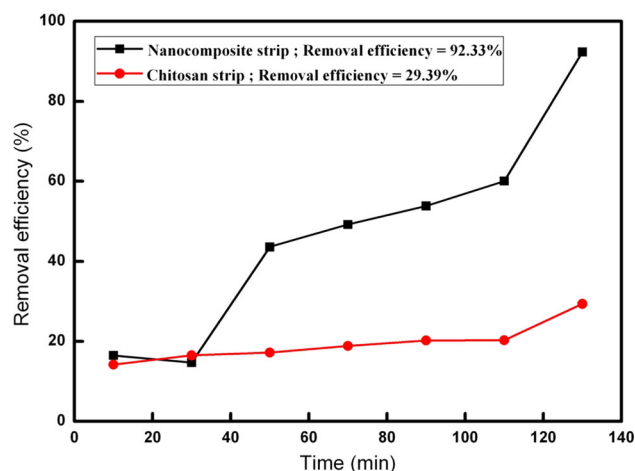


**Fig. 13** Graph showing the removal efficiency of chitosan strip and chitosan-magnetite nanocomposite with relation to time

$E = (C_0 - C_t/C_0) \times 100$ . Therefore, the nanocomposite strip enhances 62.94 % than the chitosan strip.

### Mechanism of adsorption and chromium removal

Adsorption is a mass transfer process in which a substance is transferred from the liquid phase to the surface of a solid. Chitosan is a biopolymer that has protonated amine groups, hydroxyl and carboxylates, which serve as active binding sites for metal ions (Guibal 2004).  $Fe_3O_4$  nanoparticles are negatively charged and have large surface area leading to increased adsorption efficiency (Nirmala 2014). Negatively charged  $Fe_3O_4$  nanoparticles bind to chitosan, which is positively charged to form chitosan-magnetite nanocomposite (Xiaowang Liu et al. 2008). Chromium(VI) exists in aqueous solutions as  $Cr_2O_7^{2-}$ ,  $HCrO_4^-$ ,  $CrO_4^{2-}$  and  $HCr_2O_7^-$ . When chitosan-magnetite nanocomposite strip is dropped into aqueous  $K_2Cr_2O_7$  solution, dichromate ions which are negatively charged bind with the cationic amine groups of chitosan, resulting in electrostatic attraction. This is followed by ion exchange process, where Cr(VI) ions replace the adsorbed  $H^+$  ions from  $Fe_3O_4$  surface (Shetty 2006) as described in the scheme (Fig. 14). During the redox process, Cr(VI) is reduced to Cr(III), resulting in the removal of chromium. At low pH (2–3), electrostatic attraction takes place, resulting in adsorption, and at high pH, electrostatic repulsion takes place, leading to desorption.

### Conclusion

Magnetite nanoparticles are synthesized using chemical co-precipitation method. UV-visible spectrum of magnetite nanoparticles showed the  $\lambda_{max}$  at 407 nm. The particle size

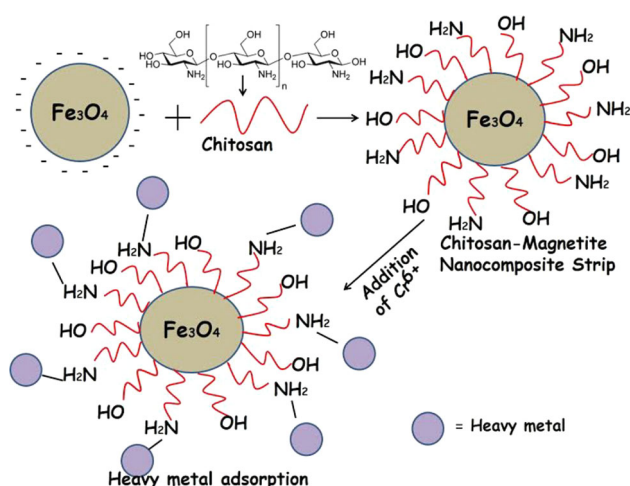


**Fig. 14** Schematic representation of mechanism behind the removal of chromium by chitosan-magnetite nanocomposite strip

was found to be 15–30 nm and spherical in shape as analysed under atomic force microscope. FTIR analysis exhibited a characteristic band at  $684\text{ cm}^{-1}$ , which is specific for Fe–O bonding to indicate the presence of  $\text{Fe}_3\text{O}_4$  nanoparticles. XRD analysis shows the diffraction peak at (311) lattice plane, which is the plane for magnetite nanoparticles. Vibrating sample magnetometer results indicated the coercivity ( $H_{ci}$ ) and retentivity ( $M_r$ ) value of magnetite nanoparticles as 61.172 Oe and 5.4324 emu/g, respectively. The magnetization value of the magnetite nanoparticles is 70.787 emu/g. From the hysteresis loop, it is confirmed that the synthesized magnetite nanoparticle is a soft magnet that can be magnetized and demagnetized quickly. From the FESEM results for the chitosan-magnetite nanocomposite strip, the elemental composition was found to be iron having a weight percentage of 52.71 %. Chitosan-magnetite nanocomposite strip and chitosan strip were evaluated for the removal of chromium from  $\text{K}_2\text{Cr}_2\text{O}_7$  (potassium dichromate) solution. The adsorption tests at different time intervals were recorded, and the removal efficiency of chitosan and chitosan-magnetite nanocomposite strip was plotted. The chromium removal efficiency of chitosan strip is 29.39 %, and that of the chitosan-magnetite nanocomposite strip is 92.33 %. Therefore, the nanocomposite strip has enhanced 62.94 % more than the control chitosan strip. Thus, it can be concluded that the removal efficiency of chromium using chitosan-magnetite nanocomposite strip is highly efficient, and studies are being performed for further improvement in treating tannery effluents.

**Acknowledgments** Vaishnavi Sureshkumar thanks UGC for providing Rajiv Gandhi Fellowship for the PG program. S C G Kiruba Daniel would like to acknowledge TNSCST, Government of Tamil Nadu, India, for RFRS funding. The authors gratefully acknowledge DST, New Delhi, Ministry of Science and Technology, Government

of India, in the form of facility project National Facility for Drug Development for Academia, Pharmaceutical and Allied Industries.

**Open Access** This article is distributed under the terms of the Creative Commons Attribution License which permits any use, distribution, and reproduction in any medium, provided the original author(s) and the source are credited.

## References

- Adikary SU, Sewvandi GA (2011) Removal of heavy metals from wastewater using chitosan, Department of Material Science and Engineering, University of Moratuwa
- Cai W, Wan J (2007) Facile synthesis of superparamagnetic magnetite nanoparticles in liquid polyols. *J Colloid Interface Sci* 305:366–370
- Campo AD, Sen T, Lellouche JP, Bruce IJ (2005) Multifunctional magnetite and silica-magnetite nanoparticles: synthesis, surface activation and application in life sciences. *J Magn Magn Mater* 293:33–40
- Chang YC, Chen DH (2005) Preparation and adsorption properties of monodisperse chitosan-bound  $\text{Fe}_3\text{O}_4$  magnetic nanoparticles for removal of Cu(II) ions. *J Colloid Interface Sci* 283:446–451
- Chen G, Hu J, Irene ML (2005) Removal and recovery of Cr (VI) from wastewater by maghemite nanoparticles. *J Hazard Mater* 2:4528–4536
- Deng YH, Wang CC, Hu JH, Yang WL, Fu SK (2005) Investigation of formation of silica-coated magnetite nanoparticles via sol-gel approach. *J Colloids Surf A Physiochem Eng Asp* 262:87–93
- Guibal E (2004) Interactions of metal ions with chitosan-based sorbents: a review. *J Sep Purif Technol* 38:43–74
- Guin D, Manorama VS (2008) Room temperature synthesis of monodispersed iron oxide nanoparticles. *J Mater Lett* 62:3139–3142
- Han Y, Lingyun Y, Zhen Y, Hu Y, Aimin L, Rongshi C (2012) Preparation of chitosan/poly(acrylic acid) magnetic composite microspheres and applications in the removal of copper(II) ions from aqueous solutions. *J Hazard Mater* 229–230:371–380
- Kim DK, Zhang Y, Voit W, Rao KV, Kehr J, Bjelke B, Muhammed M (2001) Superparamagnetic iron oxide nanoparticles for biomedical applications. *Scripta Mater* 44:1713–1717
- Liu X, Hu Q, Fang Z, Zhang X, Zhang B (2008) Magnetic chitosan nanocomposites: a useful recyclable tool for heavy metal ion removal. In: Langmuir J (ed) vol 25, pp 3–8
- Martínez-Mera I, Espinosa-Pesqueira ME, Pérez-Hernández R, Arenas-Alatorre J (2007) Synthesis of magnetite ( $\text{Fe}_3\text{O}_4$ ) nanoparticles without surfactants at room temperature. *J Mater Lett* 61:4447–4451
- McBain SC, Yiu HHP, Dobson J (2008) Magnetic nanoparticles for gene and drug delivery. *Int J Nanomed* 3:169–180
- Nirmala I (2014) Use of iron oxide magnetic nanosorbents for Cr (VI) removal from aqueous solutions: a review. *J Eng Res Appl* 4:55–63
- Pattanaik A (2011) Synthesis and characterization of amine-functionalized magnetic silica nanoparticle, Doctoral dissertation
- Rahman MM, Khan SK, Jamal A, Faisal M, Aisiri MA (2011) Iron oxide nanoparticles, Mohammed Rahman (ed) ISBN: 978-953-307-913-4 (InTech)
- Recep A, Ulvi U (2008) Adsorptive features of chitosan entrapped in polyacrylamide hydrogel for  $\text{Pb}^{2+}$ ,  $\text{UO}_2^{2+}$ , and  $\text{Th}^{4+}$ . *J Hazard Mater* 151:380–388
- Shetty AR (2006) Metal anion removal from wastewater using chitosan in a polymer enhanced diafiltration system, A Thesis



- submitted to the Faculty of Worcester Polytechnic Institute, Degree of Master of Science in Biotechnology
- Shilpi K, Padmaja PS, Sudhakar (2011) Adsorption of mercury(II), methyl mercury(II) and phenyl mercury(II) on chitosan cross-linked with a barbitol derivative. *Carbohydr Polym* 86:1055–1062
- Sundrarajan M, Ramalakshmi M (2012) Novel cubic magnetite nanoparticle synthesis using room temperature ionic liquid. *J Chem* 9:1070–1076
- Waldon RD (2008) Infrared spectra of ferrites. *J Phys Rev* 1955(99):1727
- Xu P, Zengam GM, Huang DH, Feng CL, Hu S, Zhao MH, Lai C, Wei Z, Huang C, Xie GX, Liu ZF (2012) Use of iron oxide nanomaterials in wastewater treatment. *J Sci Total Envir* 424:1–10
- Yuan P, Liu D, Fan M, Yang D, Zhu R, Ge F, Zhu JX, He HP (2010) Removal of hexavalent chromium [Cr(VI)] from aqueous solutions by the diatomite-supported/unsupported magnetite nanoparticles. *J Hazard Mater* 173:614–621
- Yue W, Zhiru T, Yi C, Yuexia G (2011) Adsorption of Cr(VI) from aqueous solutions using chitosan-coated fly ash composite as biosorbent. *Chem Eng J* 175:110–116
- Zheng W, Li XM, Yang Q, Zeng GM, Shen XX, Zhang J, Liu JJ (2007) Adsorption of Cd(II) and Cu (II) from aqueous solution by carbonate hydroxyapatite derived from egg shell waste. *J Hazard Mater* 147:534–539